

Cdc55 coordinates spindle assembly and chromosome disjunction during meiosis

Farid Bizzari and Adele L. Marston

Wellcome Trust Centre for Cell Biology, School of Biological Sciences, University of Edinburgh, Edinburgh EH9 3JR, Scotland, UK

During meiosis, two consecutive nuclear divisions follow a single round of deoxyribonucleic acid replication. In meiosis I, homologues are segregated, whereas in meiosis II, sister chromatids are segregated. This requires that the sequential assembly and dissolution of specialized chromosomal factors are coordinated with two rounds of spindle assembly and disassembly. How these events are coupled is unknown. In this paper, we show, in budding yeast, that the protein phosphatase 2A regulatory subunit Cdc55 couples the loss of

linkages between chromosomes with nuclear division by restraining two other phosphatases, Cdc14 and PP2A^{Rts1}. Cdc55 maintains Cdc14 sequestration in the nucleolus during early meiosis, and this is essential for the assembly of the meiosis I spindle but not for chromosomes to separate. Cdc55 also limits the formation of PP2A holocomplexes containing the alternative regulatory subunit Rts1, which is crucial for the timely dissolution of sister chromatid cohesion. Therefore, Cdc55 orders passage through the meiotic divisions by ensuring a balance of phosphatases.

Introduction

Meiosis produces haploid gametes from diploid cells through two consecutive nuclear divisions without an intervening DNA replication phase. The first division, meiosis I, which is termed reductional, separates the paternal and maternal chromosomes or homologues. Meiosis II, which is reminiscent of mitosis, is called equational because the identical sister chromatids are separated. Compared with mitosis, three changes to the chromosomes ensure sequential reductional and equational segregation in meiosis (Marston and Amon, 2004). First, uniquely in meiosis I, sister chromatids attach to microtubules emanating from the same spindle pole (monoorientation), rather than opposite poles (biorientation) as in mitosis and meiosis II. In budding yeast, the monopolin complex, which associates with kinetochores during meiosis I, is thought to fuse sister kinetochores together to ensure monoorientation, though its function is not conserved (Tóth et al., 2000; Hauf and Watanabe, 2004; Yokobayashi and Watanabe, 2005; Petronczki et al., 2006; Gregan et al., 2007; Monje-Casas et al., 2007; Sakuno and Watanabe, 2009; Corbett et al., 2010). Second, homologues are linked during meiosis I, most commonly by chiasmata, the products of meiotic recombination, to allow the generation of tension upon the attachment of homologues to opposite poles. Third, sister chromatid

cohesion is lost in two steps during meiosis. During meiosis I, separase-dependent cleavage of the meiosis-specific Rec8 subunit of cohesin on chromosome arms resolves chiasmata and triggers the reductional segregation of homologues, but centromeric cohesin is protected until separase is reactivated during meiosis II. Centromeric cohesin is protected because Shugoshin (Sgo1) recruits protein phosphatase 2A (PP2A), a trimeric enzyme consisting of a scaffold (A), regulatory (B), and catalytic (C) subunit to centromeres, and this antagonizes Rec8 phosphorylation, which is a prerequisite for its cleavage (Clift and Marston, 2011). Although alternative PP2A A, B, and C subunits allow for the assembly of several distinct holoenzymes (Virshup and Shenolikar, 2009), only PP2A containing the B' regulatory subunit (Rts1 in budding yeast) protects centromeric Rec8 (Kitajima et al., 2006; Riedel et al., 2006; Tang et al., 2006).

Furthermore, modified cell cycle controls ensure that two rounds of nuclear division occur without an intervening S phase during meiosis. One essential feature of meiosis is the sequential assembly of meiosis I and meiosis II spindles within the same cell, but how this is orchestrated is unknown. During mitosis, spindle elongation is followed by cell cycle exit, which is characterized by inactivation of Cdk5, spindle disassembly, and

Correspondence to Adele L. Marston: adele.marston@ed.ac.uk

Abbreviations used in this paper: PP2A, protein phosphatase 2A; qPCR, quantitative PCR; SAC, spindle assembly checkpoint; tdTomato, tandem dimer Tomato.

© 2011 Bizzari and Marston. This article is distributed under the terms of an Attribution-Noncommercial-Share Alike-No Mirror Sites license for the first six months after the publication date (see <http://www.rupress.org/terms>). After six months it is available under a Creative Commons License (Attribution-Noncommercial-Share Alike 3.0 Unported license, as described at <http://creativecommons.org/licenses/by-nc-sa/3.0/>).

cytokinesis (Sullivan and Morgan, 2007). It is thought that at the meiosis I to meiosis II transition, only a partial down-regulation of Cdks occurs to allow spindle disassembly but not complete cell cycle exit, but the mechanism may differ between organisms (Marston and Amon, 2004).

A key regulator of the meiosis I to meiosis II transition in budding yeast is the Cdc14 phosphatase (Buonomo et al., 2003; Marston et al., 2003). Cdc14 function is best understood in mitosis, in which it plays an essential role in mitotic exit through dephosphorylation of key substrates to promote Cdk inactivation and coordinate late mitotic events (Stegmeier and Amon, 2004). Before anaphase, Cdc14 is bound to its inhibitor Cfi1/Net1 in the nucleolus, an interaction promoted by the dephosphorylation of Cfi1 by PP2A containing the Cdc55 B regulatory subunit (Queralt et al., 2006). At anaphase onset, separase activation, as part of the nonessential Cdc14 early anaphase release network (Rock and Amon, 2009), down-regulates PP2A^{Cdc55} (Queralt et al., 2006; Queralt and Uhlmann, 2008), allowing Cdks to phosphorylate Cfi1. This disrupts the Cfi1–Cdc14 interaction, triggering Cdc14 release from the nucleolus (Azzam et al., 2004). Sustained Cdc14 release and Cdk inactivation require the activity of a second essential network called the mitotic exit network (Shou et al., 1999; Visintin et al., 1999). Because separase both triggers cohesin loss and down-regulates PP2A^{Cdc55}, Cdc14 early anaphase release–dependent Cdc14 release couples chromosome segregation to mitotic exit (Queralt et al., 2006).

We have explored the roles of PP2A^{Cdc55} in meiosis. We find that Cdc55-depleted cells undergo a very delayed and inefficient single meiotic division, in which chromosome segregation is near random. The misregulation of two other phosphatases, Cdc14 and PP2A^{Rts1}, accounts for this phenotype. Cdc55 is required to prevent ectopic Cdc14 release early in meiosis to allow spindle assembly. Cdc55 additionally limits the cellular levels of PP2A containing the alternative B' regulatory subunit Rts1, thereby ensuring the timely cleavage of Rec8 by separase. Our findings show that, by maintaining a balance of phosphatases, Cdc55 is a key coordinator of the meiotic program.

Results

Cells lacking Cdc55 undergo a single mixed meiotic division

We analyzed a strain in which *CDC55* is under control of the meiotically repressed *CLB2* promoter (*cdc55mn* for *cdc55 meiotic null*), resulting in Cdc55 depletion during meiosis (Clift et al., 2009). Although wild-type cells completed both meiotic divisions efficiently (~90% tetranucleate cells; Fig. 1 A), a single nuclear division occurred in only ~20% of *cdc55mn* cells, and tetranucleate cells were not observed (Fig. 1 B). A *cdc55Δ* strain behaved similarly (Fig. 1 C). We used strains that produce tetracycline repressor–GFP and in which *tetO* arrays are integrated close to the centromere of one copy of chromosome V (heterozygous *CEN5*-GFP) to examine the segregation of sister chromatids. Heterozygous *CEN5*-GFP foci were found in the same nucleus of virtually all wild-type binucleate cells, whereas ~35% of binucleate *cdc55mn* or *cdc55Δ* cells had *CEN5*-GFP foci in both nuclei, indicating equational (meiosis II–like)

segregation (Fig. 1 D). To examine homologue segregation in *cdc55mn* cells, we used strains with *CEN5*-GFP on both copies of chromosome V (homozygous *CEN5*-GFP). Although GFP label was found in both nuclei in 100% of wild-type binucleate cells, homologue segregation in *cdc55mn* cells was essentially random, as ~50% of Cdc55-depleted binucleate cells lacked any GFP label in one of the nuclei (Fig. 1 E).

Impaired nuclear division in Cdc55-depleted cells is not caused by unresolved linkages between chromosomes because ablating linkages genetically did not restore nuclear division. *SPO11*, which is required for chiasmata formation (Keeney et al., 1997), *MAM1*, encoding a monopolin subunit (Tóth et al., 2000), and *REC8*, encoding a meiosis-specific cohesin subunit (Klein et al., 1999), were deleted in *cdc55mn* cells alone and in combination. However, none of these deletions improved nuclear division in *cdc55mn* cells nor did they radically alter the frequency (~30%) of binucleate cells with heterozygous *CEN5*-GFP in both nuclei or homozygous *CEN5*-GFP in one nucleus (~50%; Fig. S1). Only deletion of *REC8* slightly increased the percentage of *spo11Δ cdc55mn* binucleate cells with either heterozygous or homozygous *CEN5*-GFP foci in both nuclei (Fig. S1). This indicates that only cohesin-dependent linkages contribute to the segregation pattern of *cdc55mn* cells.

Cdc55 controls the nucleolar localization of Cdc14 phosphatase during meiosis

During mitosis, Cdc55 promotes the nucleolar sequestration of Cdc14 (Queralt et al., 2006). We monitored Cdc14 localization during meiosis using a pachytene block–release protocol to obtain synchronized cultures (Fig. 1, F and G; Carlile and Amon, 2008). In wild-type cells, Cdc14 was released from the nucleolus in two waves, coinciding with the appearance of anaphase I and anaphase II spindles (Fig. 1 F; Buonomo et al., 2003; Marston et al., 2003). In *cdc55mn* cultures, however, Cdc14 release occurred prematurely, before spindle assembly (Fig. 1 G). Indeed, meiosis I spindle assembly was extremely delayed in *cdc55mn* cells, and meiosis II spindles were rarely observed (Fig. 1 G).

We analyzed Cdc14 localization (Cdc14-GFP) and spindle morphology (GFP-Tub1) in live cells undergoing meiosis (Matos et al., 2008). To restrict our analysis to cells with a known history, we examined cells with GFP-Tub1 localization typical of prophase I at the start of filming and in which Cdc14 was released from the nucleolus at least once during the observation period. In the wild-type example in Fig. 1 H (arrows indicate sequestered Cdc14-GFP; also see Video 1), a metaphase I spindle forms, and nucleolar Cdc14-GFP signal disappears immediately preceding anaphase I spindle elongation. Cdc14-GFP nucleolar foci reappear in the daughter nuclei and, subsequently, dissipate just before anaphase II (Fig. 1 H). In contrast, *cdc55mn* cells in which Cdc14-GFP release occurred after prophase I exhibited several kinds of behaviors (Fig. 1, I–K). In the majority of cells (330/563; Fig. 1 I and Video 2), Cdc14-GFP was released from its bright nucleolar spot and remained released until the end of filming, though neither spindle assembly nor nuclear division occurred. The remainder of cells attempted to make a spindle, resequestered Cdc14-GFP, or divided their nuclei (Fig. 1 K). Interestingly, 80/90 *cdc55mn*

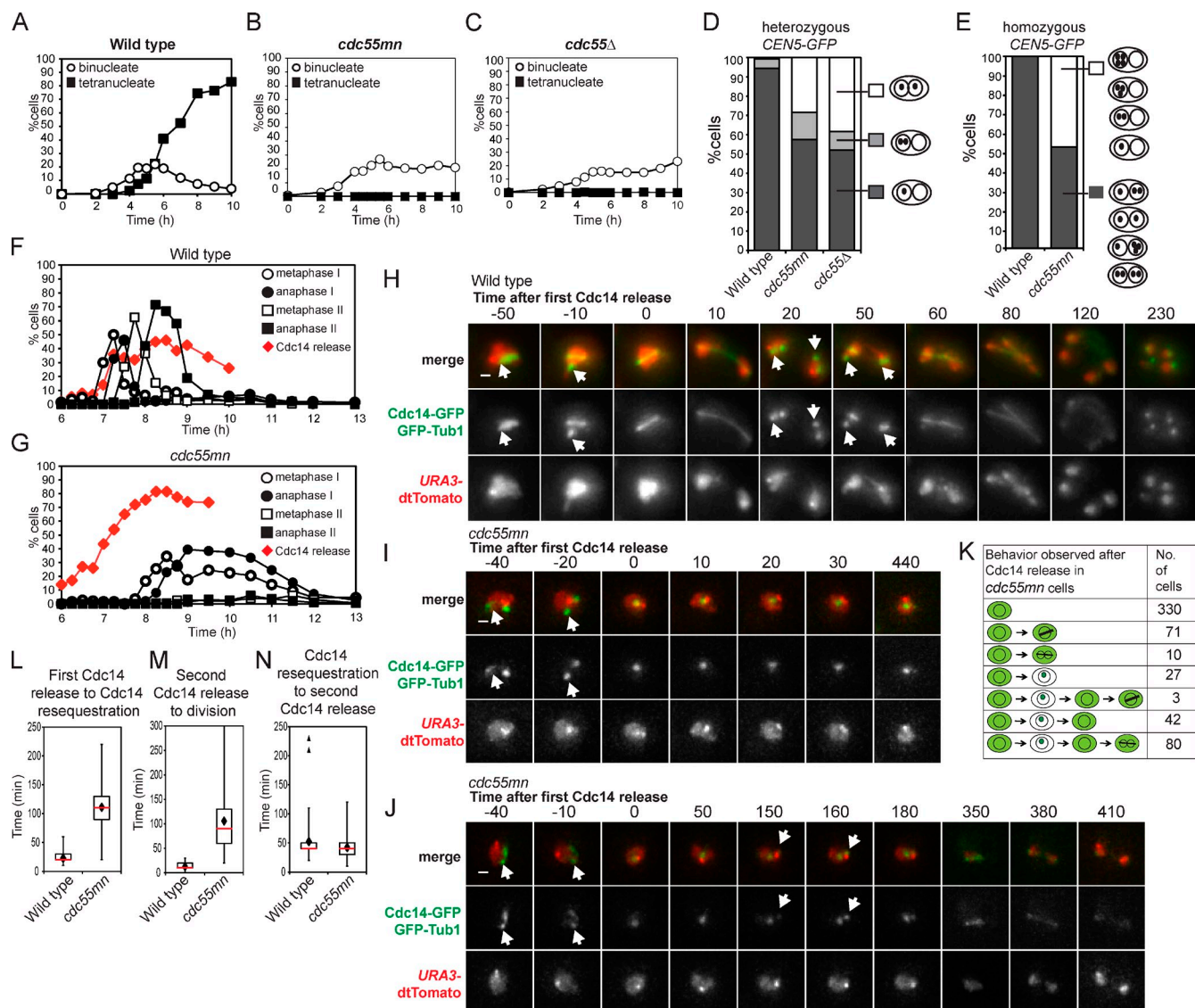


Figure 1. Impaired nuclear division, random chromosome segregation, and ectopic Cdc14 release in *cdc55mn* cells. (A–D) Meiosis was induced in strains carrying heterozygous *CEN5-GFP*, *PDS1-18MYC*, and otherwise wild type (AM4796), *cdc55mn* (AM4891), or *cdc55Δ* (AM5338). The percentages of binucleate and tetranucleate cells ($n = 200$; A–C) or the pattern of GFP foci in binucleate cells ($n > 800$; D) is shown for a representative experiment. (E) Wild-type (AM6040) and *cdc55mn* (AM5936) strains carrying homozygous *CEN5-GFP* were analyzed as described in D. (F and G) Wild-type (AM6633) and *cdc55mn* (AM6626) cells carrying 3HA-CDC14, GAL-NDT80, and *pGPD1-GAL4(848)ER* were induced to sporulate and released from a pachytene block at 6 h. The percentages of cells with the indicated spindle morphology and with Cdc14 released from the nucleolus are shown for a representative experiment. (H–K) Wild-type (AM6935) and *cdc55mn* (AM6942) cells carrying *CDC14-GFP*, *GFP-TUB1*, and homozygous *terR-dTomato* were filmed. (H–J) Still images from Videos 1 (wild-type; H), 2 (*cdc55mn*; I), and 3 (*cdc55mn*; J). Arrows indicate Cdc14 sequestered in the nucleolus. Bars, 1 μ m. (K) Behavior of *cdc55mn* cells that were in prophase I (as judged by spindle morphology) at the start of filming and released Cdc14 from the nucleolus (563/1,203 prophase I cells). Examples of extruding microtubules are shown in fixed cells in Fig. S2. Times are given in minutes. (L–N) The time elapsed between the first Cdc14 release to Cdc14 resequestration (L), the second Cdc14 release to nuclear division (M), or Cdc14 resequestration and rerelease (N) are shown for cells that were in prophase I at the start of filming and in which two rounds of Cdc14 release were observed (wild type, $n = 95$; *cdc55mn*, $n = 80$). Box boundaries represent the bottom quartile and top quartile. The red line indicates the median, diamonds indicate the mean, and error bars represent the minimum and maximum values observed except for in the case of N in which two outliers (triangles) were excluded from the analysis. Because images were captured at 10-min intervals, the time elapsed between two observed events is subject to an error of 20 min.

cells that divided their nuclei resequestered Cdc14 before this division (Fig. 1 J and Video 3). In these 80 *cdc55mn* cells that underwent two rounds of Cdc14-GFP release, both the first (Fig. 1 L) and second (Fig. 1 M) round of release, though not the period of resequestration (Fig. 1 N), were on average extended compared with wild type. These observations confirmed that Cdc55 is essential to prevent Cdc14 release until after spindle formation. When spindles form in *cdc55mn* cells, this is commonly preceded by

Cdc14 resequestration, suggesting that nuclear division may occur at the usual time of meiosis II.

Cohesin loss from chromosomes in the absence of spindle assembly in *cdc55mn* cells

We asked whether failed spindle assembly in *cdc55mn* cells prevents the loss of linkages between chromosomes. During meiosis,

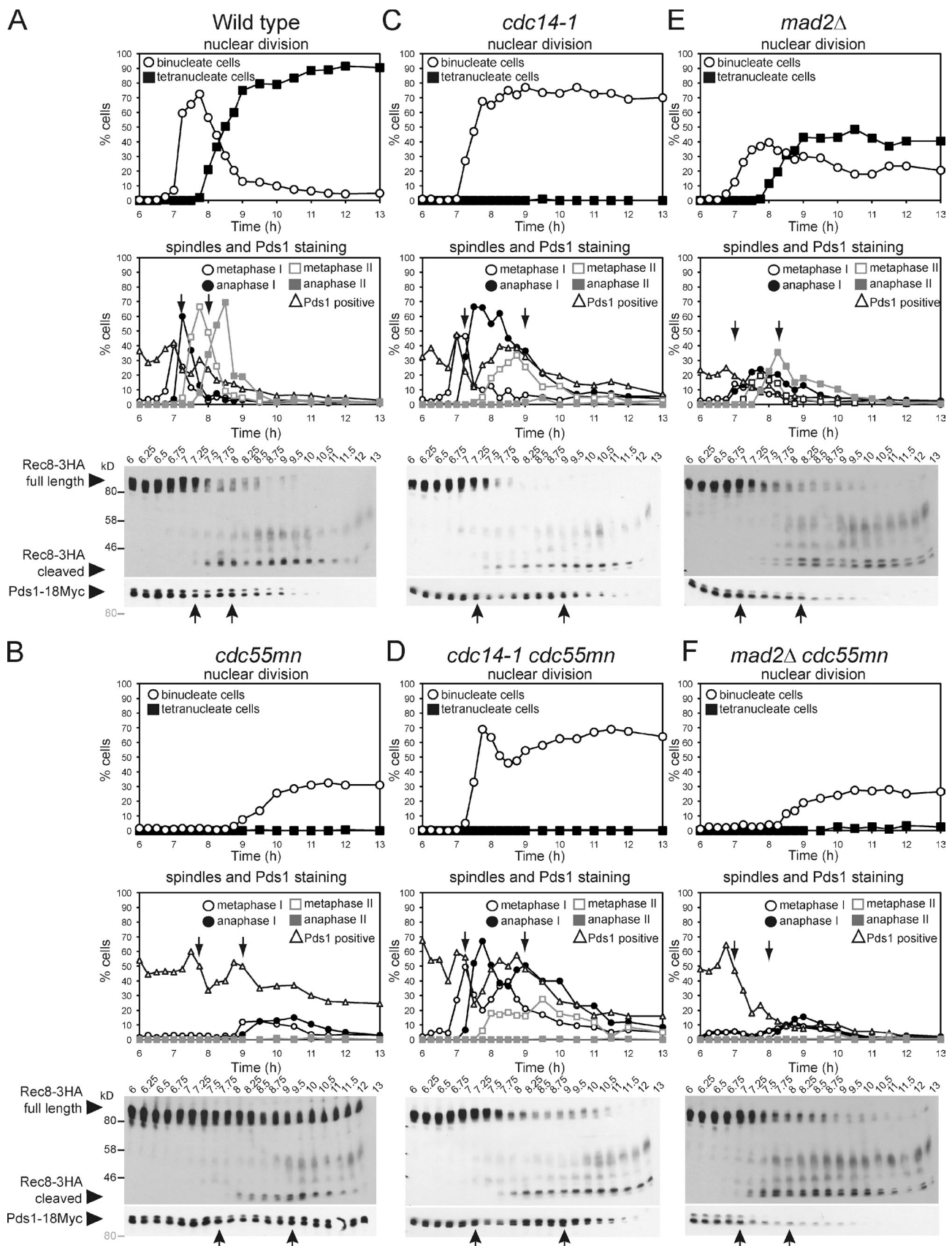


Figure 2. Impaired spindle assembly in *cdc55mn* cells is caused by ectopic Cdc14 activation. (A-F) Wild-type (AM6142; A), *cdc55mn* (AM6131; B), *cdc14-1* (AM7549; C), *cdc14-1 cdc55mn* (AM7550; D), *mad2Δ* (AM7547; E), and *mad2Δ cdc55mn* (AM7548; F) strains carrying *REC8-3HA*, *PDS1-18MYC*, *GAL-NDT80*, and *pGPD1-GAL4(848)*. ER were cultured as described in Fig 1 (F and G). The percentages of binucleate and tetranucleate cells,

the separase inhibitor securin (Pds1) is destroyed in two waves during anaphase I and anaphase II, liberating separase to cleave the chromosomal arm and centromeric cohesin (Rec8), respectively. We compared the timing of Pds1 degradation and Rec8 cleavage with spindle assembly in *cdc55mn* cells. In wild-type cells, as expected, the first round of Pds1 degradation coincided with a reduction in full-length Rec8, appearance of a shorter cleavage product, and the accumulation of anaphase I spindles and binucleate cells (Fig. 2 A). In *cdc55mn* cells, bulk Pds1 degradation was delayed, and although Rec8 cleavage occurred soon afterward, neither anaphase I spindles nor nuclear division formed at this time (Fig. 2 B), although extruding and fragmented microtubules were observed (Fig. S2). Nuclear division was instead coupled to the second round of Pds1 degradation in *cdc55mn* cells (Fig. 2 B). Consistent with the two waves of Pds1 degradation, Rec8 was lost from chromosome arms first and then centromeres later in *cdc55mn* cells (Fig. S2). These results indicate that the stepwise loss of cohesin is preserved in *cdc55mn* cells but uncoupled from spindle formation, which occurs only at the time expected for meiosis II. Because linkages between chromosomes are already lost at the time of nuclear division, this explains the near-random segregation of *cdc55mn* cells.

Premature Cdc14 activation prevents spindle assembly in *cdc55mn* cells

To determine whether ectopic Cdc14 release is the reason for delayed and inefficient spindle formation in *cdc55mn* cells, we introduced the temperature-sensitive *cdc14-1* allele into *cdc55mn* cells. At the restrictive temperature (30°C), *cdc14-1* mutants assemble robust meiosis I spindles and undergo nuclear division to produce binucleate cells, though tetranucleate cells are not produced because of a failure to properly exit meiosis I (Marston et al., 2003). Nevertheless, Pds1 undergoes two cycles of accumulation and destruction, and Rec8 cleavage is stepwise in *cdc14-1* cells, with nuclear division and the appearance of anaphase I spindles being coupled to the first round of Pds1 degradation (Fig. 2 C; Marston et al., 2003). Remarkably, metaphase I spindles assembled with normal timing in *cdc14-1 cdc55mn* cells, and the first round of Pds1 destruction and Rec8 cleavage were coupled to the appearance of anaphase I spindles (Fig. 2 D). Therefore, spindle assembly fails in *cdc55mn* cells as a result of the ectopic activation of Cdc14.

Inactivation of Cdc14 not only rescued the spindle assembly defect of *cdc55mn* cells but also partially alleviated the delay in Pds1 destruction. Pds1 stabilization in *cdc55mn* cells might occur because the absence of a spindle would inevitably result in unattached kinetochores that could engage the spindle assembly checkpoint (SAC). Indeed, in cells lacking *MAD2*, which is required for a functional SAC (Shonn et al., 2000), Pds1 degradation and Rec8 cleavage were initiated with similar timing

whether or not Cdc55 was present (7 h; Fig. 2, E and F). For reasons that are unclear, the percentage of Pds1-positive cells in the pachytene arrest (6 h) were higher in *cdc55mn* cultures, independent of *MAD2* or *CDC14*. Nevertheless, these findings indicate that ectopic Cdc14 activation in *cdc55mn* cells prevents spindle assembly, which leads to activation of the SAC.

Although inactivation of Cdc14 or Mad2 alleviated the delay to the first wave of Pds1 destruction and Rec8 cleavage in *cdc55mn* cells, full-length Rec8 was present at later time points in cultures in which Cdc55 was depleted (Fig. 2, C–F). This suggested that Cdc55 might also have Cdc14-independent roles in ensuring timely cleavage of cohesin during meiosis II.

Inactivation of Cdc14 in *cdc55mn* cells rescues homologue, but not sister, segregation

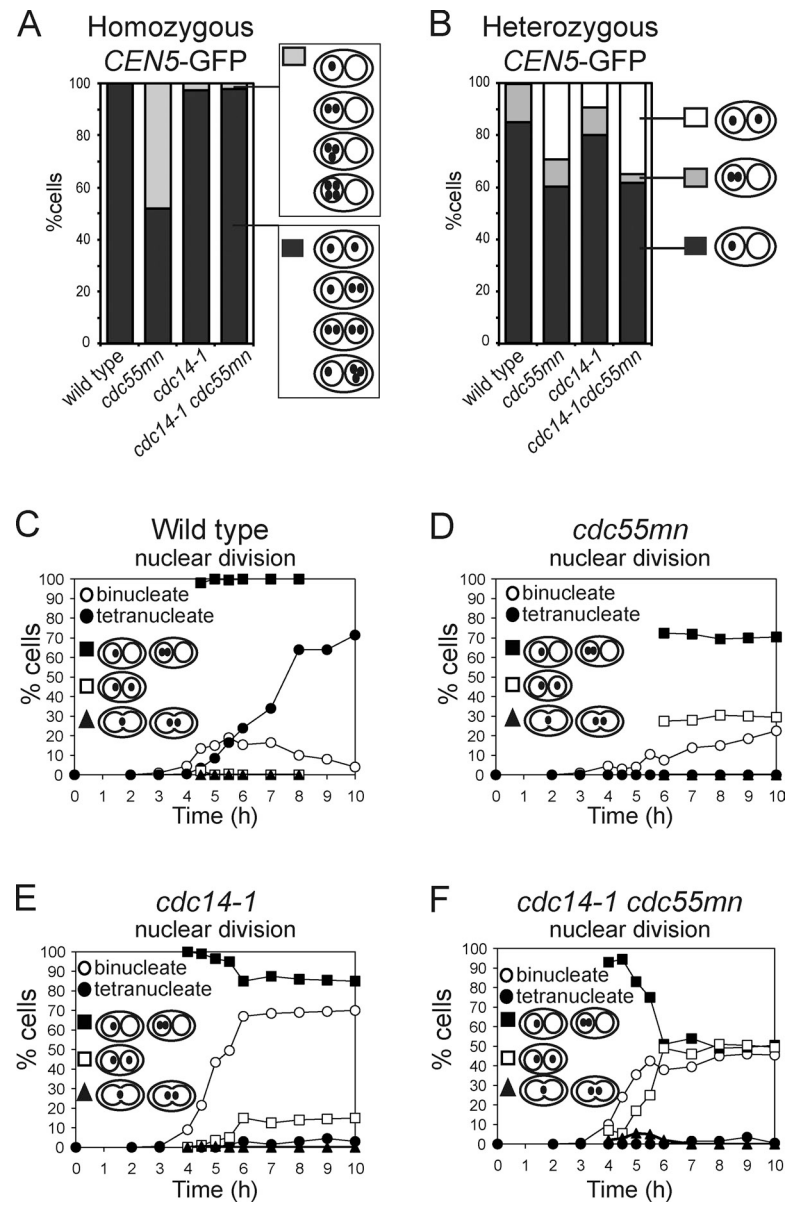
We took advantage of the *cdc14-1* background to ask whether defective spindle assembly alone accounted for the missegregation of chromosomes in *cdc55mn* cells. Examination of homozygous *CEN5*-GFP dots showed that homologue segregation in the *cdc55mn* strain was rescued by inactivation of Cdc14 because the GFP label was found in both nuclei of virtually all *cdc14-1 cdc55mn* binucleate cells (Fig. 3 A). Analysis of heterozygous *CEN5*-GFP foci revealed that, surprisingly, inactivation of Cdc14 did not reduce the frequency of equational segregation in *cdc55mn* cells (Fig. 3 B). We found previously that the *cdc14-1* mutant undergoes a normal reductional meiosis I but that, subsequently, a fraction (10–15%) of sister chromatids segregate equationally on the same axis during meiosis II (Marston et al., 2003). We asked whether a similar increase in equational segregation occurs over time in *cdc14-1 cdc55mn* cells. As expected, virtually all wild-type binucleate cells from all time points analyzed had a heterozygous *CEN5*-GFP label in just one nucleus (Fig. 3 C), whereas ~30% of binucleate *cdc55mn* cells had a GFP label in both nuclei (Fig. 3 D). Consistent with previous results (Marston et al., 2003), the first binucleate cells to appear in *cdc14-1* cultures had a GFP label in one nucleus and only later were up to ~10% of cells observed with a GFP label in both nuclei (Fig. 3 E). In *cdc14-1 cdc55mn* cells, segregation of *CEN5*-GFP to the same nucleus was also observed first; however, the frequency of subsequent segregation to opposite nuclei was greatly increased, up to ~50% (Fig. 3 F). These results indicate that Cdc55 has effects on chromosome segregation that are independent of its role in controlling Cdc14.

The spindle assembly defect in *cdc55mn* cells is not caused by premature Clb1 degradation

We investigated how ectopically activated Cdc14 prevents spindle assembly in *cdc55mn* cells. During exit from mitosis, Cdc14 triggers the inactivation of Cdks, largely by promoting cyclin

Pds1-positive cells, and cells with the indicated spindle morphology were determined. Anti-HA and anti-Myc immunoblots showing the positions of full-length Rec8-3HA, cleaved Rec8-3HA, and Pds1-18Myc (arrowheads) are shown with protein molecular mass markers in black (anti-HA) or gray (anti-Myc). Arrows indicate a reduction in Pds1-positive cells in the first and second meiotic division. Blots are representative (A and B) or were performed once (C–F). Numbers at the top of the blots indicate time in hours.

Figure 3. The *cdc14-1* mutation rescues homologue segregation in *cdc55mn* cells but does not prevent equational segregation on the same axis. (A) Segregation of homozygous *CEN5-GFP* foci in $\geq 1,000$ binucleate cells of wild-type (AM6040), *cdc55mn* (AM5936), *cdc14-1* (AM6902), and *cdc14-1 cdc55mn* (AM6908) strains were determined as described in Fig. 1 D. (B–F) Segregation of heterozygous *CEN5-GFP* in wild-type (AM4796), *cdc55mn* (AM4891), *cdc14-1* (AM6910), and *cdc14-1 cdc55mn* (AM6934) cells. (B) Segregation in binucleate cells was determined as described in A. (C–F) The total percentage of binucleate and tetranucleate cells and the percentage of binucleate cells that have GFP foci in one, both, or between the two nuclei are shown for a representative experiment.



destruction, and this is a prerequisite for spindle disassembly (Sullivan and Morgan, 2007). During meiosis, metaphase I spindle assembly correlates with the appearance of Cdk activity associated with the cyclins Clb1 and Clb4 (Carlile and Amon, 2008), and Clb1 is retained in the nucleus of *cdc14-1* cells during meiosis (Marston et al., 2003). We tested whether ectopically released Cdc14 in *cdc55mn* cells prevents Clb1 nuclear accumulation. In wild-type cells, the presence of a meiosis I-specific slower migrating Clb1 form, thought to represent the active kinase-associated form (Carlile and Amon, 2008), correlated with Clb1 nuclear localization (Fig. 4 A). In *cdc14-1* cells, Clb1 export from the nucleus was delayed, though it lost its nuclear enrichment and converted to the faster migrating form as cells entered anaphase I, indicating that Cdc14, surprisingly, is not required for these changes (Fig. 4 B). In *cdc55mn* cells, Clb1 export from the nucleus and conversion to the faster migrating form was abolished (Fig. 4 C), arguing against the idea that ectopically active Cdc14 inactivates Clb1 in *cdc55mn* cells. Indeed,

in the *cdc14-1 cdc55mn* mutant, loss of Clb1 nuclear enrichment and conversion to the faster migrating form occurred with similar kinetics to wild type (Fig. 4 D). Therefore, the critical role of Cdc14 in meiosis I exit appears not to be the nuclear export of Clb1. Moreover, the spindle assembly defect of *cdc55mn* cells is not caused by a failure to concentrate Clb1 in the nucleus.

Spindle midzone proteins do not prevent spindle assembly in *cdc55mn* cells

We considered whether three proteins, Ase1, Fin1, and Sli15 (INCENP), which are known to be dephosphorylated by Cdc14 during anaphase and affect spindle stability, prevent spindle assembly in *cdc55mn* cells. Dephosphorylation by Cdc14 during anaphase causes Ase1 to focus to the spindle midzone, Fin1 to associate with microtubules, and Sli15 to be recruited to the spindle midzone (Pereira and Schiebel, 2003; Woodbury and Morgan, 2006; Khmelinskii et al., 2007). We reasoned that ectopic Cdc14 in *cdc55mn* cells could result in

the premature conversion of Ase1, Fin1, or Sli15 to the unphosphorylated form with the potential to interfere with spindle assembly. If this were true, inactivation of *ASE1*, *FIN1*, or *SLI15* would be expected to rescue the spindle assembly defect of *cdc55mn* cells, provided that these mutations did not by themselves preclude spindle assembly during meiosis. However, deletion of *ASE1* or *FIN1* did not rescue spindle formation or nuclear division in *cdc55mn* cells, whereas both *ase1Δ* and *fin1Δ* cells built metaphase I spindles efficiently (Fig. S3). Because Sli15 targets the Aurora B kinase (Ipl1 in budding yeast) to the spindle, we examined a strain depleted for Ipl1 in meiosis (*ipl1mn*). Although spindle assembly was impaired in Ipl1-depleted cells as seen in other systems (Sampath et al., 2004; Colombié et al., 2008), codepletion of Cdc55 resulted in a more severe spindle assembly defect (Fig. S3). Therefore, mistargeting one of the Cdc14 substrates, Ase1, Fin1, or the Sli15-associated kinase Ipl1, does not prevent spindle assembly in *cdc55mn* cells.

Kinetochores are monooriented in *cdc55mn* cells, but sister segregation is delayed

Next, we asked why depletion of Cdc55 increases equational segregation in the *cdc14-1* background. One explanation could be that during meiosis I, sister kinetochores fail to attach to microtubules from the same spindle pole body (monoorientation) and attach to microtubules from opposite poles (biorientation) instead. This would lead to the equational segregation of sister chromatids only once centromeric cohesion is lost at meiosis II. Indeed, *CDC55* was previously identified in a screen to uncover new components of the monopolin complex that specifies monoorientation during meiosis I (Rabitsch et al., 2003). However, analysis of the monopolin subunit Mam1 on spread meiotic nuclei indicated that it was recruited to and disappeared from kinetochores with similar timing to that in wild type in *cdc55mn* cells (Fig. 5, A–D). We monitored the splitting of heterozygous *CEN5*-GFP foci that occurs only when sister kinetochores are bioriented in metaphase I-arrested cells (by depletion of the anaphase-promoting complex activator Cdc20; Lee and Amon, 2003). Because the absence of spindles in *cdc55mn* cells precludes *CEN5*-GFP separation even when sister kinetochores are bioriented (Fig. S4), we conducted this experiment in the *cdc14-1* background. In *cdc20mn cdc14-1* control cells, little sister centromere separation was observed, as sister kinetochores are monooriented, whereas deletion of *MAM1* resulted in *CEN5*-GFP separation in up to 50% of cells (Fig. S4). Similarly, a high frequency of sister centromere separation was observed in *cdc14-1 mam1Δ cdc55mn* cells (although not to the same level as a *cdc14-1 mam1Δ* for unknown reasons; Fig. S4). The frequency of centromere splitting was lower in *cdc14-1 cdc55mn* cells with intact *MAM1*, indicating that kinetochore monoorientation is at least partially functional in *cdc55mn* cells (Fig. S4). To further address this issue, we assessed the contribution of monopolin to the segregation pattern of *cdc55mn* cells with a spindle (Fig. S4 and Fig. 5, E–H). Deletion of *MAM1* in either the *cdc14-1* or *cdc14-1 cdc55mn* strain resulted in the equational segregation of heterozygous *CEN5*-GFP foci in the majority of

binucleate cells (Fig. 5, G and H), arguing that the majority of sister kinetochores monoorient in *cdc55mn* cells. Furthermore, binucleate cells with partially divided nuclei and GFP foci trapped in the middle were prevalent in the *cdc14-1 mam1Δ cdc55mn* but not in the *cdc14-1 mam1Δ* culture (Fig. 5, G and H). These observations indicate that Cdc55 is not required for kinetochore monoorientation but rather suggest that Cdc55 promotes the timely resolution of sister chromatids at meiosis II.

Two rounds of spindle assembly in *cdc14-1* cells depleted for Cdc55

The finding that Cdc55 is required for the timely separation of sister chromatids at meiosis II suggested that persistent linkages between sister chromatids might be the cause of the increased equational segregation caused by depletion of Cdc55 in *cdc14-1* cells. To gain a clearer picture of the timing of equational segregation, we examined heterozygous GFP dot segregation in *cdc14-1* and *cdc14-1 cdc55mn* cells in synchronized cells. In *cdc14-1* cells, anaphase I spindles appeared after 7.25 h; however, binucleate cells with *CEN5*-GFP in both nuclei did not accumulate until 8.5 h (Fig. 6 A). In *cdc14-1 cdc55mn* cells, surprisingly, after the anaphase I peak declined, it gave way to a second metaphase I peak followed by a second anaphase I peak, which correlated with the equational segregation of *CEN5*-GFP (Fig. 6 B). The unexpected two rounds of spindle assembly and disassembly in *cdc14-1 cdc55mn* cells were also observed in other synchronized experiments and were reflected as a transient decline in the numbers of binucleate cells at the time expected for meiosis I exit (e.g., Figs. 2 D and 4 D). Interestingly, two similar, but less pronounced, peaks were observed in synchronized cultures of the *cdc14-1* single mutant, although anaphase I spindles tended to disassemble into spindles with metaphase II-like morphology, which probably represent two half-spindles (Fig. 6 A; also see Figs. 2 C and 4 B). These findings infer that, contradicting the interpretation of experiments with poorly synchronized cultures in which meiosis I and meiosis II cannot be resolved (Buonomo et al., 2003; Marston et al., 2003), spindle disassembly does occur after meiosis I in the absence of Cdc14 function, only to reassemble along the same axis.

To visualize the relationship between spindle behavior and equational segregation in real time, we filmed live *cdc14-1* and *cdc14-1 cdc55mn* cells carrying GFP-Tub1 and heterozygous *URA3*-tandem dimer Tomato (tdTomato; ~35 kb from *CEN5*; Fig. 6, C–E). In the majority (64%) of *cdc14-1* cells in which nuclear division was observed after prophase I, only a single division occurred, after which two short spindles appeared, as shown in the example in Fig. 6 C and Video 4. However, *cdc14-1 cdc55mn* cells performed two nuclear divisions on the same axis with a high frequency (82%; Fig. 6 D and Video 5). Remarkably, as inferred from the fixed samples (Fig. 6 B), spindles underwent elongation followed by disassembly, reassembly, and reelongation that correlated with nuclear division, refusion, and then redvision, respectively (Fig. 6 D and Video 5). This behavior was also observed in *cdc14-1* cells with a lower frequency (36%). Although we cannot rule out the possibility that *cdc14-1* cells retain residual Cdc14 activity that is

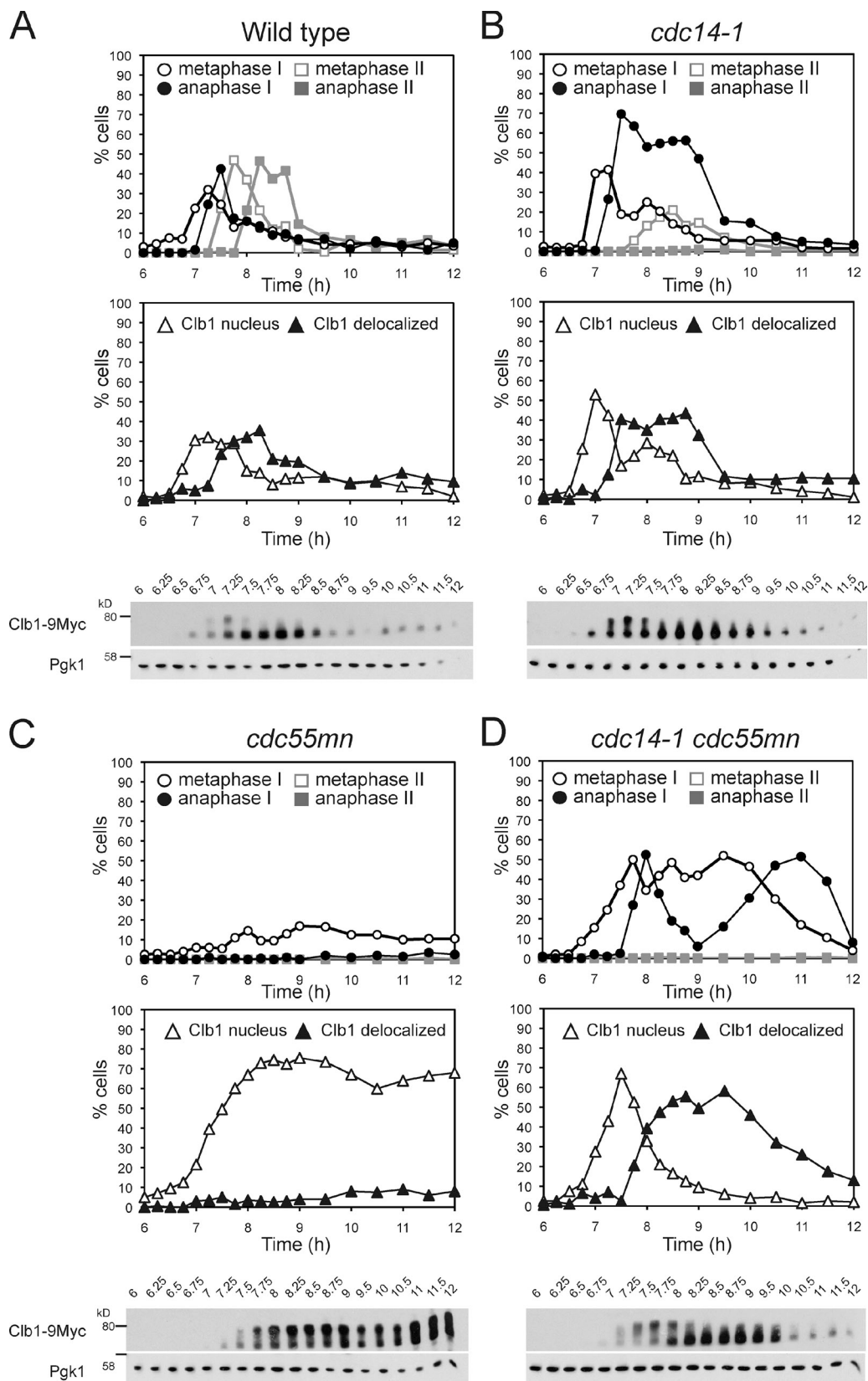


Figure 4. Ectopic Cdc14 activation does not cause premature degradation of the meiotic cyclin Clb1. (A–D) Wild-type (AM6770; A), *cdc14-1* (AM7815; B), *cdc55mn* (AM6961; C), and *cdc14-1 cdc55mn* (AM7816; D) cells carrying *CLB1-9MYC*, *GAL-NDT80*, and *pGPD1-GAL4(848)ER* were released from a pachytene arrest. The percentages of cells with the indicated spindle morphology (top) or *Clb1-9Myc* localization (middle) were determined at the indicated time points. The anti-Myc immunoblot (bottom) is shown with the anti-Pgk1 immunoblot as a loading control and the positions of molecular mass markers indicated. Western blots are representative (A and C) or were performed once (B and D). Numbers at the top of the blots indicate time in hours.

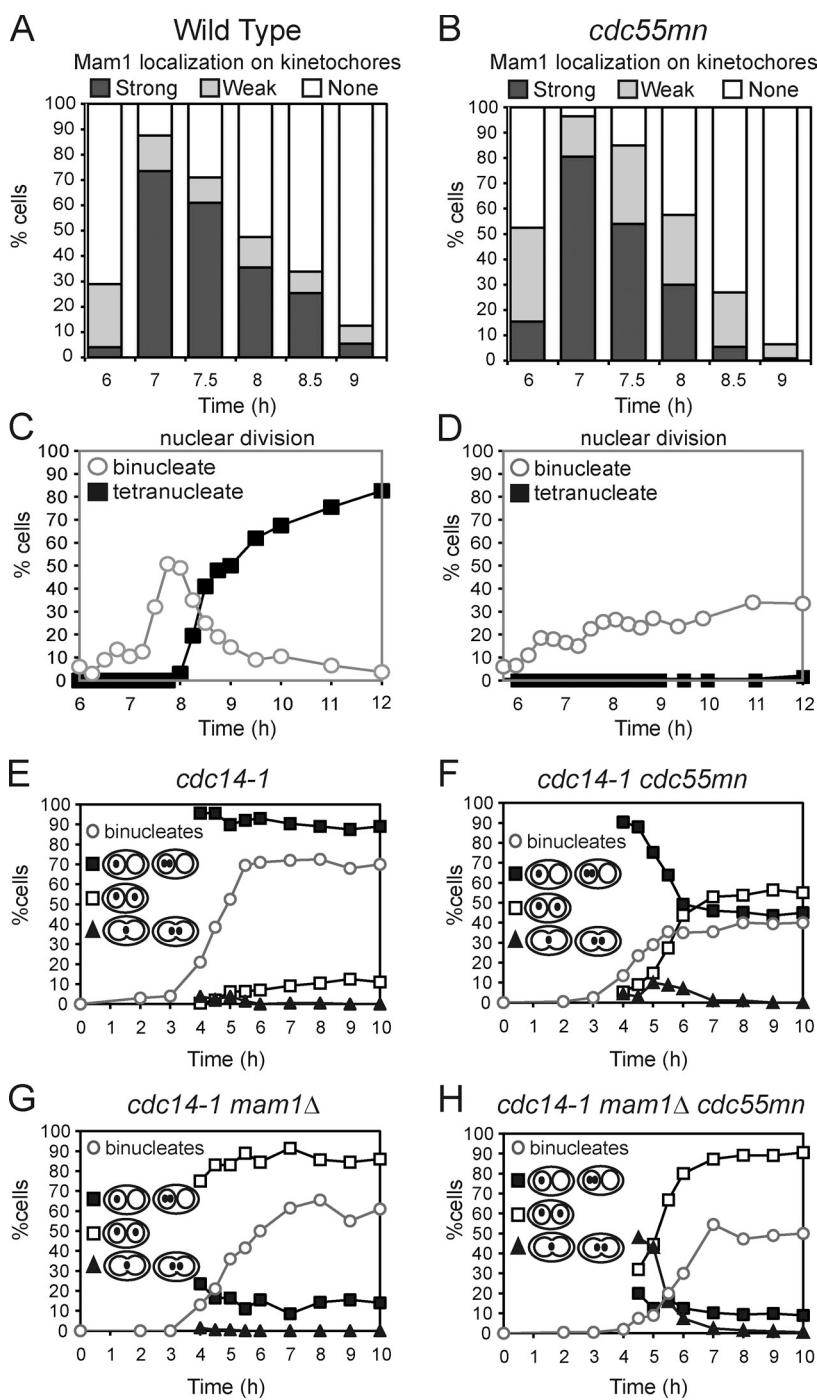


Figure 5. Kinetochores are monooriented during meiosis I in *cdc55mn* cells. (A–D) Wild-type (AM5901; A and C) and *cdc55mn* (AM5771; B and D) cells carrying *MAM1-9MYC*, *NDC10-6HA*, *GAL-NDT80*, and *pGPD1-GAL4(848)ER* were released from a pachytene block, and the localization of Mam1-9Myc was determined using Ndc10-6HA as a marker for kinetochores. (C and D) The percentages of binucleate and tetranucleate cells determined at the indicated time points are shown for a representative experiment. (E–H) Strains carrying heterozygous *CEN5-GFP* dots and otherwise *cdc14-1* (AM6910), *cdc14-1 cdc55mn* (AM6934), *cdc14-1 mam1Δ* (AM7355), and *cdc14-1 mam1Δ cdc55mn* (AM7328) were analyzed as described in Fig. 3 (C–F).

sufficient for spindle breakdown, the ability of these cells to build robust meiosis I spindles in the *cdc55mn* background suggests that this is unlikely. Importantly, in both *cdc14-1* and *cdc14-1 cdc55mn* strains, in which a single division was observed, it was usually reductional, whereas when a second division occurred, it was most often equational and was preceded by a reductional division (Fig. 6 E). This confirms that reductional and equational segregations occur sequentially on the same axis in *cdc14-1* cells. Interestingly, the time taken for the second division tended to be longer in cells depleted for Cdc55 (Fig. 6 F). This raises the possibility that difficulty in resolving linkages between chromosomes in *cdc55mn* cells causes partially divided

nuclei to recoalce, which increases the probability of equational segregation at the time of meiosis II.

What could be the nature of the persistent linkages between chromosomes that cause nuclei to refuse in *cdc14-1 cdc55mn* cells? Removal of chiasmata by deletion of *SPO11* abolishes the second peak of anaphase I spindles and equational segregation in *cdc14-1* cells, suggesting that residual linkages between homologues could be responsible (Fig. 6 G; Marston et al., 2003). However, we found that deletion of *SPO11* did not abolish the second anaphase I peak and only partially decreased the incidence of equational segregation in *cdc14-1 cdc55mn* cells (Fig. 6 H). This suggests that both interhomologue and intersister

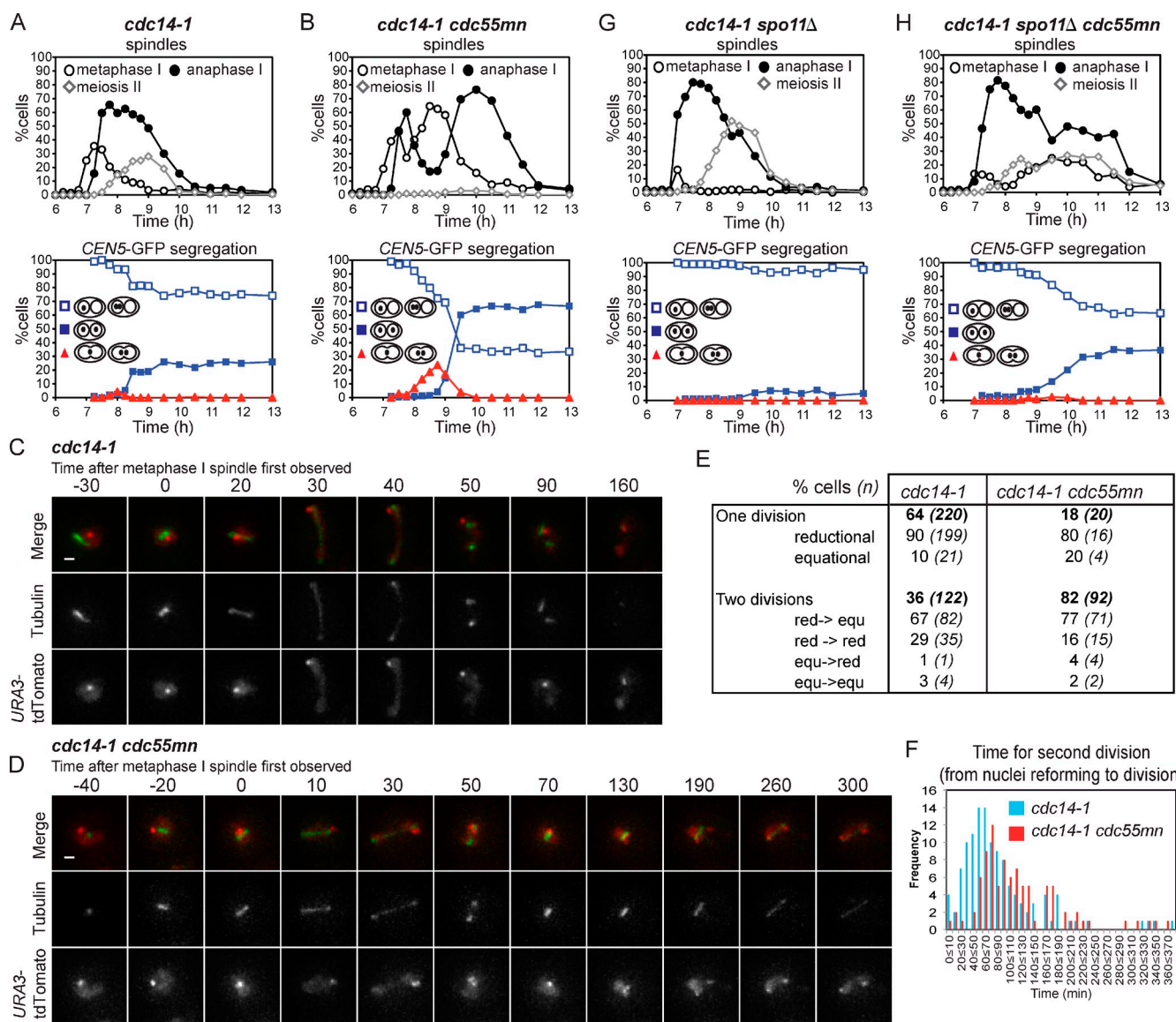


Figure 6. Equational segregation occurs on a newly assembled spindle in *cdc14-1* mutants and is elevated by Cdc55 depletion. (A and B) Strains carrying heterozygous *CEN5-GFP*, *GAL-NDT80*, *pGPD1-GAL4(848).ER*, and either *cdc14-1* (AM8044; A) or *cdc14-1 cdc55mn* (AM8045; B) were released from a pachytene block, and the percentages of cells with the indicated spindle morphology (top graph) and pattern of *CEN5-GFP* localization in the binucleate cells (bottom graph) were determined. (C–F) *cdc14-1* (AM7866) and *cdc14-1 cdc55mn* (AM7867) cells carrying *URA3-tdTomato* (red) and *GFP-TUB1* (green) were imaged at 10-min intervals for a total of 9 h and 46 min and 9 h and 56 min, respectively. (C) Example of a *cdc14-1* cell that completes a single meiotic division. (D) Example of a *cdc14-1 cdc55mn* cell that completes two divisions on the same axis. Times at the top are given in minutes. Bars, 1 μ m. (E) Behavior of *cdc14-1* and *cdc14-1 cdc55mn* cells that were initially in prophase I and which performed at least one division during the course of filming. red, reductional; equ, equational. (F) The frequency of *cdc14-1* and *cdc14-1 cdc55mn* cells that performed the second division within the indicated time period. Also see Videos 4 and 5. (G and H) Strains carrying heterozygous *CEN5-GFP* dots *GAL-NDT80*, *pGPD1-GAL4(848).ER*, and either *spo11Δ* *cdc14-1* (AM8046; G) or *spo11Δ cdc14-1 cdc55mn* (AM8047; H) were treated as described in A and B.

linkages play a part in nuclear refusion and in increasing the frequency of equational segregation in *cdc14-1 cdc55mn* cells.

Persistent centromeric cohesion increases equational segregation in *cdc55mn* cells

Two lines of evidence indicate that the overprotection of cohesin could provide the persistent linkages between sister chromatids in *cdc55mn* cells. First, Rec8 is slow to be removed from centromeres in *cdc55mn* cells (Fig. S2). Second, full-length, faster migrating Rec8 persists after the second round of securin degradation in *cdc14-1 cdc55mn* and *mad2Δ cdc55mn* cells (Fig. 2, D and F),

suggesting that it is the unphosphorylated form that is resistant to separase-dependent cleavage. Cohesin is protected by the recruitment of PP2A complexed with the alternative regulatory subunit Rts1 (PP2A^{Rts1}) to the pericentromere by Sgo1 (Clift and Marston, 2011). Consistent with the persistence of Rec8 at centromeres (Fig. S2), we found that Sgo1 removal from centromeres was delayed in *cdc55mn* cells (Fig. 7, A–F). To ask whether overprotection of Rec8 by Sgo1 causes equational segregation in *cdc14-1 cdc55mn* cells, we depleted Sgo1 in meiotic cells and analyzed the segregation of heterozygous *CEN5-GFP* in binucleate cells. Remarkably, *CEN5-GFP* segregation was reductional in virtually

all *cdc14-1 sgo1mn cdc55mn* binucleate cells (Fig. 7 G). Depletion of Sgo1 prevents equational segregation caused by the abolishment of cohesin protection rather than some other function of Sgo1 because replacement of Rec8 by the mitotic cohesin Scc1, which is refractory to Sgo1-PP2A^{Rts1} protection (Tóth et al., 2000), also abolished equational segregation in *cdc14-1 cdc55mn* cells (Fig. 7 H). Furthermore, the accumulation of metaphase I spindles in *cdc14-1 cdc55mn* cells was abolished by either Sgo1 depletion or replacement of Rec8 by Scc1 (Fig. S5). We conclude that overprotection of cohesin precludes the timely resolution of linkages to allow equational segregation on the same axis during meiosis I in *cdc14-1 cdc55mn* mutants.

An imbalance of PP2A isoforms in *cdc55mn* cells

Why is the deprotection of cohesin delayed in Cdc55-depleted cells? Because Cdc55 and Rts1 are alternative regulatory (B) subunits for PP2A, we considered that the absence of Cdc55 might lead to an excess of PP2A scaffold (A) and catalytic (C) subunits available to associate with Rts1. This, in turn, could result in the recruitment of high levels of PP2A^{Rts1} to centromeres and the persistence of unphosphorylated, noncleavable cohesin. Indeed, more Rts1 coimmunoprecipitated with the PP2A A subunit Tpd3 in extracts from *cdc55mn* cells than from wild-type cells undergoing meiosis (Fig. 7 I). We used chromatin immunoprecipitation followed by quantitative PCR (qPCR) to measure the levels of Rts1 associated with four sites on chromosome IV in metaphase I-arrested cells (*cdc20mn*). Although we observed a moderate enrichment of Rts1 at the centromere-proximal site in wild-type cells, levels did not significantly rise over background at other sites examined (Fig. 7 J). In *cdc55mn* cells, however, Rts1 was highly enriched at all sites tested (Fig. 7 J), including a site on the chromosome arm (95 kb to left) where cohesin would not normally be protected during meiosis I (Kiburz et al., 2005). Similar observations were made for Sgo1 (unpublished data). We conclude that depletion of Cdc55 during meiosis causes an increase in the amount of PP2A^{Rts1} at centromeres, which overprotects cohesion.

Discussion

Cdc55 coordinates meiosis by regulating two other phosphatases

Cdc55 is a member of a conserved family of regulatory (B) subunits for PP2A (Shi, 2009). We have shown that Cdc55 plays a critical role in the coordination of the meiotic divisions in budding yeast. In the absence of Cdc55, nuclear division is impaired, and chromosomes segregate randomly. This phenotype is explained by the misregulation of two other phosphatases, Cdc14 and PP2A, in complex with the alternative regulatory subunit Rts1 (B'). Cdc55 is required to prevent the unscheduled release of Cdc14 from the nucleolus, and this, in turn, prevents spindle assembly during meiosis I but not the events triggering loss of linkages between chromosomes. Also, in the absence of Cdc55, Rts1 is highly enriched at centromeres, and this dominantly inhibits the separation of sister chromatids at meiosis II. The model in Fig. 8 illustrates how these two activities of Cdc55 couple the

loss of linkages between chromosomes to spindle assembly. We postulate that, as in mitosis (Queralt et al., 2006), separase both cleaves cohesin and down-regulates Cdc55, thereby triggering Cdc14 release. The essential role of Cdc14 in meiosis I exit is generation of a new spindle axis for meiosis II. In this way, separase activation couples meiosis I chromosome segregation to the formation of two separate spindles for meiosis II.

Regulation of Cdc14 function is essential for meiosis

These findings have established the importance of Cdc14 control during meiosis and demonstrated a crucial regulatory role of Cdc55. Cdc55 is essential for Cdc14 sequestration during early meiosis, in contrast to mitosis, in which inappropriate release of Cdc14 was observed only in metaphase-arrested *cdc55Δ* cells (Queralt et al., 2006). This difference could be because active Clb1-Cdk and Clb2-Cdk complexes, which can phosphorylate Cfi1/Net1 to promote Cdc14 release (Azzam et al., 2004), accumulate late in mitosis (Grandin and Reed, 1993). Although Clb2 is not present in meiosis, Clb1-Cdk activity accumulates soon after exit from pachytene (Carlile and Amon, 2008). Consistent with this interpretation, Cdc14 release (Fig. 1 G) in *cdc55mn* cells correlates with Clb1 accumulation in the nucleus (Fig. 4 C). Therefore, during early meiosis, the potential for Cdc14 release exists because of the presence of active Clb1-Cdk, and this places a critical requirement on PP2A^{Cdc55} to restrain Cdc14 activity.

Premature release of Cdc14 in *cdc55mn* cells prohibits meiosis I spindle assembly; similarly, treatment of mouse oocytes with okadaic acid, an inhibitor of PP2A, also prevented spindle assembly (Lu et al., 2002). Although Cdc14 homologues are not required for mitotic exit in mammals (Moccia and Schiebel, 2010), they are important for the meiosis I to meiosis II transition in mouse oocytes (Schindler and Schultz, 2009). Therefore, PP2A^{Cdc55}-dependent regulation of Cdc14 might also ensure timely spindle assembly in mouse meiosis. The mechanism of spindle assembly is not well understood but is known to be driven by Cdk activity (Sullivan and Morgan, 2007). Accordingly, in budding yeast, Cdc14 is thought to promote spindle breakdown at mitotic exit both by the reversal of Cdk-dependent phosphorylation and by promoting Cdk inactivation (Sullivan and Morgan, 2007; Woodruff et al., 2010). Although Clb1 regulation appears to be independent of Cdc14 during meiosis, further investigation is required to determine whether Cdc14 controls spindle dynamics through Cdk regulation in meiosis too.

Although ectopically released Cdc14 prevents spindle assembly, surprisingly, the SAC is only transiently activated, and securin is degraded after a delay. Unregulated Cdc14 in *cdc55Δ* mitotic cells similarly allows cell cycle progression upon treatment with microtubule-depolymerizing drugs (Yellman and Burke, 2006). This could be because Cdc14 is part of a mechanism to silence the SAC during anaphase of mitosis (Mirchenko and Uhlmann, 2010). Therefore, ectopically released Cdc14 is potentially doubly dangerous during meiosis because it may both prevent spindle assembly and turn off the checkpoint designed to halt the cell cycle in response to this failure.

Paradoxically, we found that spindle breakdown at meiosis I exit does not require Cdc14; instead, it is essential for duplication

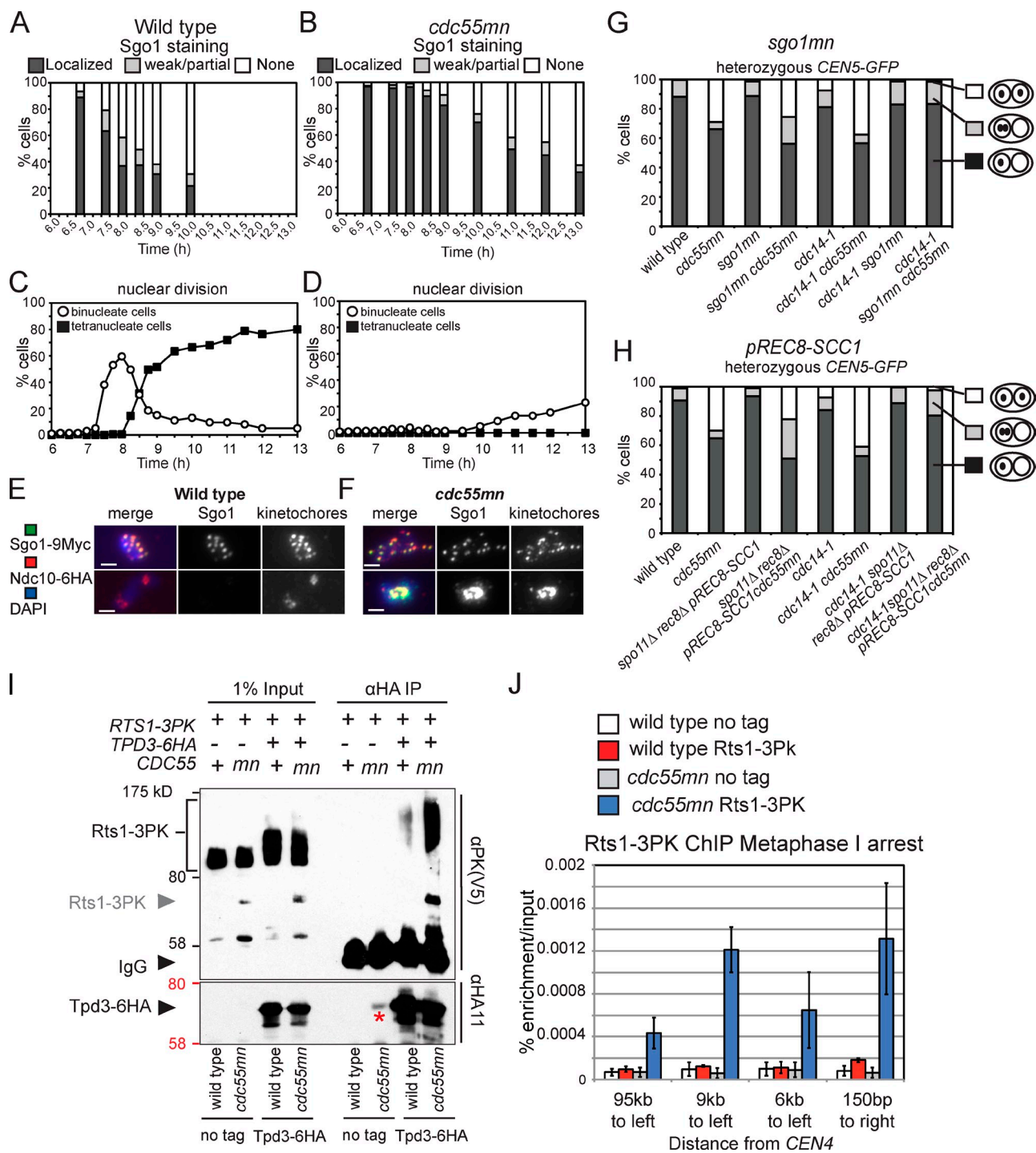


Figure 7. Overprotection of cohesin in a *cdc55mn* cell during meiosis. (A-F) Wild-type (AM7228; A, C, and E) and *cdc55mn* (AM7229; B, D, and F) cells carrying *GAL-NDT80* and *pGPD1-GAL4(848).ER* were released from the pachytene block, and Sgo1 localization at kinetochores (A and B) or the percentages of binucleate and tetranucleate cells (C and D) were determined in a single experiment. (E and F) Examples of Sgo1 localization are shown. Bars, 2 μ m. (G and H) Depletion of Sgo1 (G) or replacement of Rec8 by Scc1 (H) abolishes equational segregation in *cdc14-1 cdc55mn* cells. Strains carrying heterozygous *CEN5-GFP* and with the indicated genotypes were treated as described in Fig. 1. $n = 680-2,000$. Strains used were wild type (AM4796), *cdc55mn* (AM4891), *sgo1mn* (AM4911), *sgo1mn cdc55mn* (AM7286), *cdc14-1 cdc55mn* (AM6910), *cdc14-1 sgo1mn* (AM7360), *cdc14-1 sgo1mn cdc55mn* (AM7421), *spo11Δ rec8Δ pREC8-SCC1* (AM5501), *spo11Δ rec8Δ pREC8-SCC1 cdc55mn* (AM5502), *spo11Δ rec8Δ pREC8-SCC1 cdc14-1* (AM7361), and *spo11Δ rec8Δ pREC8-SCC1 cdc14-1 cdc55mn* (AM7362). (I) Tpd3-6HA was immunoprecipitated using anti-HA antibodies from meiotic extracts of wild-type and *cdc55mn* cells carrying *RTS1-3PK* and either *TPD3-6HA* (AM8028 and AM8014) or no tag (AM8012 and AM8029). Anti-V5 (PK) and anti-HA immunoblots of input and immunoprecipitated samples from strains of the indicated genotypes are shown, with protein molecular mass markers shown in black or red, respectively. An *Rts1-3PK* degradation product is indicated by the gray arrowhead, and the asterisk indicates residual 3HA-Cdc55. (J) qPCR analysis of chromatin immunoprecipitated using anti-V5 (PK) antibodies from *cdc20mn* (AM3560), *cdc20mn RTS1-3PK* (AM7902), *cdc20mn cdc55mn* (AM7903), and *cdc20mn cdc55mn RTS1-3PK* (AM7904) strains. The mean of three experiments is shown with error bars indicating standard deviation.

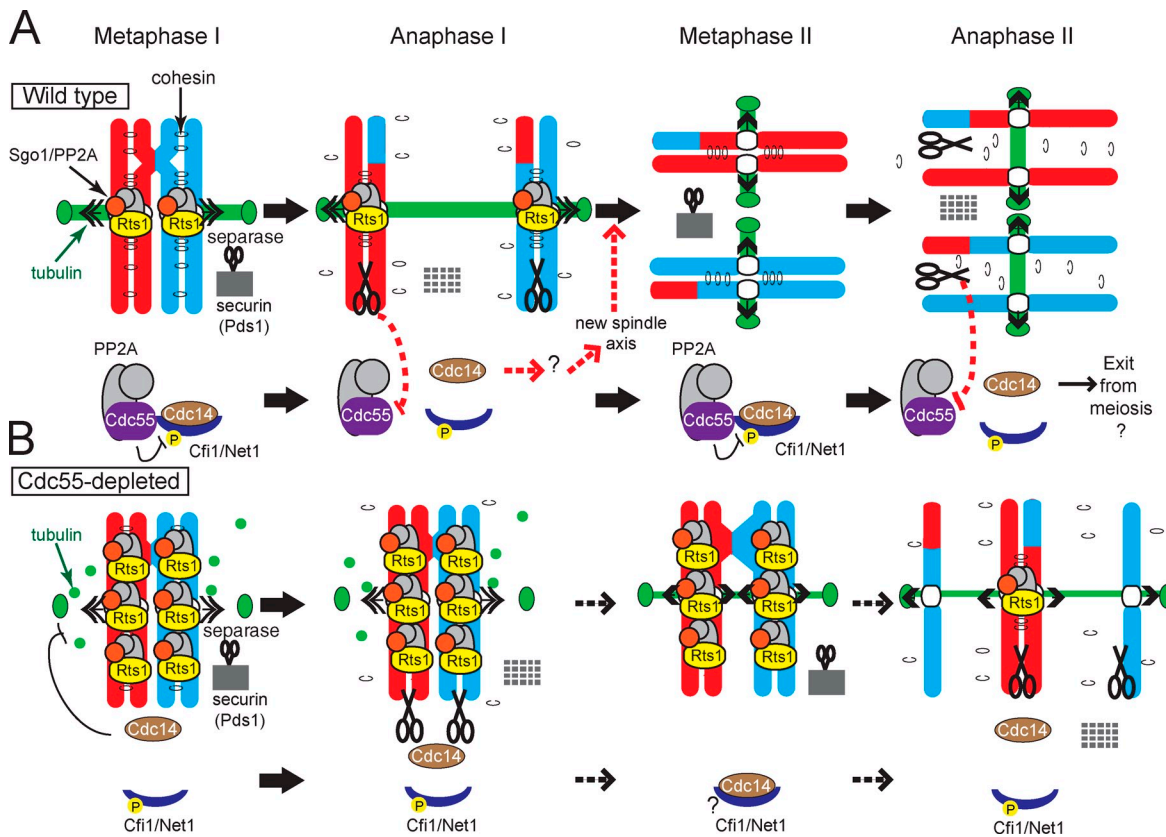


Figure 8. Model for coordination of the meiotic program by Cdc55. (A) In wild-type cells during metaphase I, PP2A^{Cdc55} both maintains Cdc14 sequestration in the nucleolus by dephosphorylating Cfi1 and restricts the amount of PP2A scaffold (A) and catalytic (C) subunits available to form a complex with Rts1 (B'). The level of PP2A^{Rts1} defines the domain of cohesion that will be protected during meiosis I. Once chromosomes are correctly aligned, separase activation leads to both the cleavage of unprotected arm cohesin and, through PP2A^{Cdc55} down-regulation, Cdc14 release. Cdc14 release during anaphase I ensures that a second spindle axis will assemble in meiosis II after its resequestration. (B) In *cdc55mn* cells, ectopic Cdc14 release interferes with spindle assembly, and excess PP2A^{Rts1} extends the domain of protected cohesin. This prevents nuclear division except in a low number of cells in which Cdc14 is relocalized to the nucleolus through an unknown mechanism (?). P indicates Cdk-dependent phosphorylation of Cfi1/Net1.

of the spindle axis. The critical function of Cdc14 is unknown, though it appears to be independent of spindle pole body duplication (unpublished data). Remarkably, the failure to build a new spindle axis allows segregated DNA masses to refuse when division is aborted as a result of unresolved linkages between chromosomes, only to undergo a second round of segregation on a new spindle built on the same axis.

Regulation of PP2A isoforms

An intriguing finding of our work is the importance of phosphatase regulatory subunits in maintaining the cellular homeostasis of PP2A isoforms. Alternate regulatory subunits confer a high degree of substrate specificity to PP2A enzymes (Virshup and Shenolikar, 2009), and our findings indicate that they also control the balance of the different isoforms. The interdependence of PP2A regulatory subunits described here for meiosis is probably widespread in other systems. Overexpression of PP2A regulatory subunits in *Xenopus laevis* and *Drosophila melanogaster* induces effects that could be attributed to competition with other subunits (Yang et al., 2003; Bajpai et al., 2004). Furthermore, mutations in the gene encoding the *Drosophila* B/PR55 subunit result in lagging chromosomes during anaphase (Mayer-Jaekel et al., 1993), which is similar to our observations upon depletion of its budding yeast homologue, Cdc55, during meiosis. PP2A is altered in

many human cancers, but the role of regulatory subunits has been difficult to dissect because both positive and negative effects have been previously described (Westerman and Hahn, 2008; Eichhorn et al., 2009). Our study has highlighted the need to consider dominant effects caused by an imbalance of PP2A isoforms to understand the mechanism of tumorigenesis. Protein kinases and phosphatases form an extensive interaction network (Breitkreutz et al., 2010). The interplay between phosphatases that we find to coordinate meiosis likely represents a general paradigm in cellular regulation. Understanding the nature of their regulatory interactions is an important goal for the future.

Materials and methods

Yeast strains

The strains used in this study are listed in Table S1 and are all derivatives of SK1. *pCLB2-3HA-CDC55* (*cdc55mn*) and *cdc55Δ* were previously described in Clift et al. (2009). *CEN5-GFP* dots, *pREC8-SCC1-3HA*, *NDC10-6HA*, *MAM1-9MYC*, and *PDS1-18MYC* were previously described in Tóth et al. (2000). *CLB1-9MYC* was previously described in Buonomo et al. (2003). *cdc20mn* and *ubr1Δ* were previously described in Lee and Amon (2003). *pCLB2-3HA-SGO1* (*sgo1mn*) and *mam1Δ* were previously described in Lee et al. (2004). *spo11Δ*, *rec8Δ*, and *REC8-3HA* were previously described in Klein et al. (1999). *3HA-CDC14*, *cdc14-1*, *REC8-13MYC*, and *SGO1-9MYC* were previously described in Marston et al. (2003). *GAL-NDT80* and *pGPD1-GAL4(848)ER* were previously described in Benjamin et al. (2003). *tetR-tet* and *tetO-URA3*, *GFP-TUB1*, and *CDC14-GFP* were

previously described in Matos et al. (2008). *RTS1-3PK* was previously described in Riedel et al. (2006). A one-step PCR method was used to generate *pCLB2-3HA-PL1* (*ipl1mn*; Lee and Amon, 2003), *mad2Δ*, *ase1Δ*, *fin1Δ* (Longtine et al., 1998), and *TPD3-6HA* constructs (Knop et al., 1999).

Growth conditions

For meiotic time courses, strains were grown for 16 h on YPG (1% yeast extract, 2% bactopeptone, 2.5% glycerol, and 2% agar) plates and then for 24 h onYPD4% (1% yeast extract, 2% bactopeptone, 4% glucose, and 2% agar) plates at 30°C (or room temperature for *cdc14-1* strains). Cells were then cultured inYPD (1% yeast extract, 2% bactopeptone, and 2% glucose) for 24 h and then inoculated at an OD₆₀₀ of 0.2–0.4 in YPA (1% yeast extract, 2% bactopeptone, and 1% potassium acetate) and grown overnight to an OD₆₀₀ of ≥1.8. Cells were then inoculated into sporulation medium (0.3% potassium acetate, pH 7) to an OD₆₀₀ of 1.8–1.9 and sporulated at 30°C. Pachytene block-release meiotic time courses were performed using strains in which expression of the *NDT80* gene, which is required for exit from pachytene, was induced by the addition of 1 μM estradiol 6 h after inoculation of cells into sporulation medium as previously described in Carlile and Amon (2008). Time course experiments were repeated for each genotype, and representative data from one experiment are shown, with the exception of the Western blots in Figs. 2 (C–F) and 4 (B and D), the chromosome spreads in Fig. 7 (A, B, E, and F), and the experiment in Fig. S3, which were performed only once.

Microscopy on fixed samples

Samples were analyzed on a microscope (Axioplan 2; Carl Zeiss) with a 100× Plan Fluar/1.45 NA (oil) objective lens, and images were taken using a camera (ORCA-ER; Hamamatsu Photonics) operated through Axiovision software (Carl Zeiss). Images were contrast adjusted in Photoshop (CS2; Adobe).

Nuclei were visualized in ethanol-fixed cells by DAPI staining. 200 cells were scored at each time point. Indirect immunofluorescence was performed as previously described in Visintin et al. (1999). Tubulin was visualized using a rat antibody at a 1:50 dilution and anti-rat FITC antibody at a 1:100 dilution. *Pds1-18Myc* was detected with a mouse anti-Myc antibody at a 1:250 dilution and anti-mouse Cy3 antibody at a 1:500 dilution. *3HA-Cdc14* was detected with a mouse HA antibody at a 1:250 dilution and an anti-mouse Cy3 antibody at a 1:500 dilution. *Clb1-9Myc* was detected with a mouse anti-Myc and an anti-mouse Cy3 antibody at 1:500 dilutions. For determination of spindle morphology or presence of *Pds1*, 200 cells were scored at each time point.

Chromosome spreading was performed as previously described (Loidl et al., 1998). *Rec8-13Myc* was detected with a rabbit anti-Myc antibody and an anti-rabbit FITC antibody at 1:300 dilutions. *Mam1-9Myc* was detected with a rabbit anti-Myc antibody and an anti-rabbit FITC at 1:100 dilutions. *Sgo1-9Myc* was detected with a rabbit anti-Myc antibody at a 1:800 dilution and an anti-rabbit FITC at a 1:250 dilution. *Ndc10-6HA* was detected with a mouse HA antibody at a 1:250 dilution and an anti-mouse Cy3 antibody at a 1:300 dilution. GFP-labeled chromosomes were visualized as in Klein et al. (1999).

Live-cell imaging

Meiotic cultures were shaken in sporulation media for 2–4 h and then immobilized with lectin on a glass coverslip. Cells were covered with sporulation medium and transferred to a temperature-controlled stage at 30°C on an imaging system (Deltavision Core; Applied Precision) with a microscope (IX71; Olympus) and a 100× Plan Apochromat/1.4 NA (oil) objective lens. 10–15 z sections of ~1 μm were acquired at 10-min intervals for up to 12 h with an EM charge-coupled device camera (Cascade II; Roper Scientific) operated by SoftWoRx (Applied Precision). Images were 3D-deconvolved maximum intensity projections; 2× digital zoom and contrast adjustment were performed using SoftWoRx.

Immunoblot analysis

Samples for immunoblot analysis were prepared and analyzed as previously described in Clift et al. (2009). Mouse anti-PK (V5) antibody was used at a 1:1,000 dilution.

Chromatin immunoprecipitation

Chromatin immunoprecipitation was performed as previously described in Fernius and Marston (2009) with the following modifications. Samples were harvested 7 h after inducing sporulation. Extracts were sonicated using the Bioruptor sonicator (Diagenode) for 30 × 30 s cycles with a 30-s resting on the maximum power setting. 15 μl protein G Dynabeads, rather than Sepharose Dynabeads, were used. To pull down *Rts1-3P*, 10 μl anti-PK (V5)

antibody was used. qPCR was performed using the SYBR green reagent (EXPRESS; Invitrogen) on the LightCycler (Roche). Primers for the sites “95 kb to left” are AM782, 5'-AGATGAAACTCAGGCTACCA-3', and AM783, 5'-TGCAACATCGTTAGTTCTG-3'; “9 kb to left” are AM1319, 5'-ATGATTCAATGGATTAGCC-3', and AM1320, 5'-GTCAGTCTTATGCT-GTCCC-3'; “6 kb to left” are AM1325, 5'-AACCTGTTAGGGAA-3'; and “150 bp right” are AM794, 5'-CCGAGGCTTCATAGCTA-3', and AM795, 5'-ACCGAAGGAAGAATAAGAA-3'.

Preparation of yeast lysates and protein immunoprecipitation

To prepare yeast lysates for immunoprecipitation, cells were induced to sporulate and harvested after 4 h. Pellets were washed once in cold double-distilled H₂O supplemented with 2 mM PMSF and then resuspended in 20% cell pellet volume of water supplemented with a protease inhibitor cocktail (5 μg/ml pepstatin A, antipain, chymostatin, leupeptin, E-64, aprotinin, 2 mM 4-(2-aminoethyl) benzenesulfonyl fluoride hydrochloride, 1 mM benzamidine, and 1 mM PMSF). Cells were drop frozen in liquid nitrogen, ground to powder in a mortar and pestle, resuspended in cold yeast lysis buffer (50 mM Tris-Cl, pH 7.6, 150 mM NaCl, 1% wt/vol Triton X-100, 1 mM EDTA [Hombauer et al., 2007]) supplemented with the aforementioned protease inhibitor cocktail, and then centrifuged and filtered through a 1.6-μm filter.

To pull down *Tpd3-6HA*, lysate containing 3 mg total protein was incubated with 7.5 μl anti-HA (12CA5) antibody with rotation for 30 min at 4°C, and 15 μl protein G Dynabeads were added for a further 1 h of incubation. The beads were then washed three times in cold yeast lysis buffer plus inhibitors and boiled in sample buffer for SDS-PAGE and Western blotting. *Tpd3-6HA* is fully functional (spore viability of strain AM8013 was 39/40); however, for unknown reasons, its presence increases the slower migrating forms of *Rts1-3PK*, and these preferentially coimmunoprecipitate with *Tpd3-6HA* (Fig. 7 I).

Online supplemental material

Fig. S1 shows that abolishing interchromosomal linkages does not rescue nuclear division or prevent equational segregation in *cdc55mn* cells. Fig. S2 shows that *Rec8* loss is stepwise in *cdc55mn* cells and provides examples of microtubule structures in *cdc55mn* cells. Fig. S3 shows that deletion of *ASE1* or *FIN1* or depletion of *Ipl1* does not restore spindle assembly to *cdc55mn* cells. Fig. S4 shows that kinetochores are monooriented during meiosis I in *cdc55mn* cells. Fig. S5 shows that depletion of *Sgo1* or replacement of *REC8* with *SCC1* rescues the accumulation of short spindles in *cdc14-1 cdc55mn* cells. Video 1 shows an example of *Cdc14* release in wild-type cells undergoing meiosis. Video 2 shows an example of a *cdc55mn* cell in which *Cdc14* released by nuclear division does not occur. Video 3 shows an example of a *cdc55mn* cell in which *Cdc14* is released and transiently resequestered before nuclear division occurs. Video 4 shows an example of a *cdc14-1* cell that performs a single reductional chromosome segregation. Video 5 shows an example of a *cdc14-1 cdc55mn* cell that performs sequential reductional and equational segregation along the same spindle axis. Online supplemental material is available at <http://www.jcb.org/cgi/content/full/jcb.201103076/DC1>.

We thank Angelika Amon, Kim Nasmyth, and Wolfgang Zachariae for yeast strains. We are grateful to David Kelly and Venkatesh Mallikarjun for assistance with live-cell imaging, Ken Sawin for advice on immunoprecipitation, and members of the Marston laboratory for helpful discussions.

Work in the Marston laboratory is supported by the Wellcome Trust, Scottish Universities Life Sciences Alliance, and the European Molecular Biology Organization Young Investigator program. F. Bizzari was a recipient of a studentship from the Overseas Research Students Awards Scheme.

Submitted: 15 March 2011

Accepted: 24 May 2011

References

- Azzam, R., S.L. Chen, W. Shou, A.S. Mah, G. Alexandru, K. Nasmyth, R.S. Annan, S.A. Carr, and R.J. Deshaies. 2004. Phosphorylation by cyclin B-Cdk underlies release of mitotic exit activator Cdc14 from the nucleolus. *Science*. 305:516–519. doi:10.1126/science.1099402
- Bajpai, R., K. Makhijani, P.R. Rao, and L.S. Shashidhara. 2004. *Drosophila* Twins regulates Armadillo levels in response to Wg/Wnt signal. *Development*. 131:1007–1016. doi:10.1242/dev.00980

Benjamin, K.R., C. Zhang, K.M. Shokat, and I. Herskowitz. 2003. Control of landmark events in meiosis by the CDK Cdc28 and the meiosis-specific kinase Ime2. *Genes Dev.* 17:1524–1539. doi:10.1101/gad.1101503

Breitkreutz, A., H. Choi, J.R. Sharom, L. Boucher, V. Neduvia, B. Larsen, Z.Y. Lin, B.J. Breitkreutz, C. Stark, G. Liu, et al. 2010. A global protein kinase and phosphatase interaction network in yeast. *Science.* 328:1043–1046. doi:10.1126/science.1176495

Buonomo, S.B., K.P. Rabitsch, J. Fuchs, S. Gruber, M. Sullivan, F. Uhlmann, M. Petronczki, A. Tóth, and K. Nasmyth. 2003. Division of the nucleolus and its release of CDC14 during anaphase of meiosis I depends on separase, SPO12, and SLK19. *Dev. Cell.* 4:727–739. doi:10.1016/S1534-5807(03)00129-1

Carlile, T.M., and A. Amon. 2008. Meiosis I is established through division-specific translational control of a cyclin. *Cell.* 133:280–291. doi:10.1016/j.cell.2008.02.032

Clift, D., and A.L. Marston. 2011. The role of shugoshin in meiotic chromosome segregation. *Cytogenet. Genome Res.* 133:234–242. doi:10.1159/000323793

Clift, D., F. Bizzari, and A.L. Marston. 2009. Shugoshin prevents cohesin cleavage by PP2A(Cdc55)-dependent inhibition of separase. *Genes Dev.* 23:766–780. doi:10.1101/gad.507509

Colombié, N., C.F. Cullen, A.L. Brittle, J.K. Jang, W.C. Earnshaw, M. Carmena, K. McKim, and H. Ohkura. 2008. Dual roles of Incenp crucial to the assembly of the acentrosomal metaphase spindle in female meiosis. *Development.* 135:3239–3246. doi:10.1242/dev.022624

Corbett, K.D., C.K. Yip, L.S. Ee, T. Walz, A. Amon, and S.C. Harrison. 2010. The monopolin complex crosslinks kinetochore components to regulate chromosome-microtubule attachments. *Cell.* 142:556–567. doi:10.1016/j.cell.2010.07.017

Eichhorn, P.J., M.P. Creyghton, and R. Bernards. 2009. Protein phosphatase 2A regulatory subunits and cancer. *Biochim. Biophys. Acta.* 1795:1–15.

Fernius, J., and A.L. Marston. 2009. Establishment of cohesion at the pericentromere by the Ctf19 kinetochore subcomplex and the replication fork-associated factor, Csm3. *PLoS Genet.* 5:e1000629. doi:10.1371/journal.pgen.1000629

Grandin, N., and S.I. Reed. 1993. Differential function and expression of *Saccharomyces cerevisiae* B-type cyclins in mitosis and meiosis. *Mol. Cell. Biol.* 13:2113–2125.

Gregan, J., C.G. Riedel, A.L. Pidoux, Y. Katou, C. Rumpf, A. Schleiffer, S.E. Kearsey, K. Shirahige, R.C. Allshire, and K. Nasmyth. 2007. The kinetochore proteins Pcs1 and Mde4 and heterochromatin are required to prevent merotelic orientation. *Curr. Biol.* 17:1190–1200. doi:10.1016/j.cub.2007.06.044

Hauf, S., and Y. Watanabe. 2004. Kinetochore orientation in mitosis and meiosis. *Cell.* 119:317–327. doi:10.1016/j.cell.2004.10.014

Hombauer, H., D. Weismann, I. Mudrak, C. Stanzel, T. Fellner, D.H. Lackner, and E. Ogris. 2007. Generation of active protein phosphatase 2A is coupled to holoenzyme assembly. *PLoS Biol.* 5:e155. doi:10.1371/journal.pbio.0050155

Keeney, S., C.N. Giroux, and N. Kleckner. 1997. Meiosis-specific DNA double-strand breaks are catalyzed by Spo11, a member of a widely conserved protein family. *Cell.* 88:375–384. doi:10.1016/S0092-8674(00)81876-0

Khmelinskii, A., C. Lawrence, J. Roostalu, and E. Schiebel. 2007. Cdc14-regulated midzone assembly controls anaphase B. *J. Cell Biol.* 177:981–993. doi:10.1083/jcb.200702145

Kiburz, B.M., D.B. Reynolds, P.C. Megee, A.L. Marston, B.H. Lee, T.I. Lee, S.S. Levine, R.A. Young, and A. Amon. 2005. The core centromere and Sgo1 establish a 50-kb cohesin-protected domain around centromeres during meiosis I. *Genes Dev.* 19:3017–3030. doi:10.1101/gad.1373005

Kitajima, T.S., T. Sakuno, K. Ishiguro, S. Iemura, T. Natsume, S.A. Kawashima, and Y. Watanabe. 2006. Shugoshin collaborates with protein phosphatase 2A to protect cohesin. *Nature.* 441:46–52. doi:10.1038/nature04663

Klein, F., P. Mahr, M. Galova, S.B. Buonomo, C. Michaelis, K. Nairz, and K. Nasmyth. 1999. A central role for cohesins in sister chromatid cohesion, formation of axial elements, and recombination during yeast meiosis. *Cell.* 98:91–103. doi:10.1016/S0092-8674(00)80609-1

Knop, M., K. Siegers, G. Pereira, W. Zachariae, B. Winsor, K. Nasmyth, and E. Schiebel. 1999. Epitope tagging of yeast genes using a PCR-based strategy: more tags and improved practical routines. *Yeast.* 15:963–972. doi:10.1002/(SICI)1097-0061(199907)15:10B<963::AID-YEA399>3.0.CO;2-W

Lee, B.H., and A. Amon. 2003. Role of Polo-like kinase CDC5 in programming meiosis I chromosome segregation. *Science.* 300:482–486. doi:10.1126/science.1081846

Lee, B.H., B.M. Kiburz, and A. Amon. 2004. Spo13 maintains centromeric cohesion and kinetochore coorientation during meiosis I. *Curr. Biol.* 14:2168–2182. doi:10.1016/j.cub.2004.12.033

Loidl, J., F. Klein, and J. Engebrecht. 1998. Genetic and morphological approaches for the analysis of meiotic chromosomes in yeast. *Methods Cell Biol.* 53:257–285. doi:10.1016/S0091-679X(08)60882-1

Longtine, M.S., A. McKenzie III, D.J. Demarini, N.G. Shah, A. Wach, A. Brachet, P. Philippse, and J.R. Pringle. 1998. Additional modules for versatile and economical PCR-based gene deletion and modification in *Saccharomyces cerevisiae*. *Yeast.* 14:953–961. doi:10.1002/(SICI)1097-0061(199807)14:10<953::AID-YEA293>3.0.CO;2-U

Lu, Q., R.L. Dunn, R. Angeles, and G.D. Smith. 2002. Regulation of spindle formation by active mitogen-activated protein kinase and protein phosphatase 2A during mouse oocyte meiosis. *Biol. Reprod.* 66:29–37. doi:10.1095/biolreprod66.1.29

Marston, A.L., and A. Amon. 2004. Meiosis: cell-cycle controls shuffle and deal. *Nat. Rev. Mol. Cell Biol.* 5:983–997. doi:10.1038/nrm1526

Marston, A.L., B.H. Lee, and A. Amon. 2003. The Cdc14 phosphatase and the FEAR network control meiotic spindle disassembly and chromosome segregation. *Dev. Cell.* 4:711–726. doi:10.1016/S1534-5807(03)00130-8

Matos, J., J.J. Lipp, A. Bogdanova, S. Guillot, E. Okaz, M. Junqueira, A. Shevchenko, and W. Zachariae. 2008. Dbf4-dependent CDC14 kinase links DNA replication to the segregation of homologous chromosomes in meiosis I. *Cell.* 135:662–678. doi:10.1016/j.cell.2008.10.026

Mayer-Jaekel, R.E., H. Ohkura, R. Gomes, C.E. Sunkel, S. Baumgartner, B.A. Hemmings, and D.M. Glover. 1993. The 55 kd regulatory subunit of *Drosophila* protein phosphatase 2A is required for anaphase. *Cell.* 72:621–633. doi:10.1016/0092-8674(93)90080-A

Mirchenko, L., and F. Uhlmann. 2010. Sli15(INCENP) dephosphorylation prevents mitotic checkpoint reengagement due to loss of tension at anaphase onset. *Curr. Biol.* 20:1396–1401. doi:10.1016/j.cub.2010.06.023

Mocciaro, A., and E. Schiebel. 2010. Cdc14: a highly conserved family of phosphatases with non-conserved functions? *J. Cell Sci.* 123:2867–2876. doi:10.1242/jcs.074815

Monje-Casas, F., V.R. Prabhu, B.H. Lee, M. Boselli, and A. Amon. 2007. Kinetochore orientation during meiosis is controlled by Aurora B and the monopolin complex. *Cell.* 128:477–490. doi:10.1016/j.cell.2006.12.040

Pereira, G., and E. Schiebel. 2003. Separase regulates INCENP-Aurora B anaphase spindle function through Cdc14. *Science.* 302:2120–2124. doi:10.1126/science.1091936

Petronczki, M., J. Matos, S. Mori, J. Gregan, A. Bogdanova, M. Schwickart, K. Mechthler, K. Shirahige, W. Zachariae, and K. Nasmyth. 2006. Monopolar attachment of sister kinetochores at meiosis I requires casein kinase 1. *Cell.* 126:1049–1064. doi:10.1016/j.cell.2006.07.029

Queralt, E., and F. Uhlmann. 2008. Separase cooperates with Zds1 and Zds2 to activate Cdc14 phosphatase in early anaphase. *J. Cell Biol.* 182:873–883. doi:10.1083/jcb.200801054

Queralt, E., C. Lehane, B. Novak, and F. Uhlmann. 2006. Downregulation of PP2A(Cdc55) phosphatase by separase initiates mitotic exit in budding yeast. *Cell.* 125:719–732. doi:10.1016/j.cell.2006.03.038

Rabitsch, K.P., M. Petronczki, J.P. Javerzat, S. Genier, B. Chwalla, A. Schleiffer, T.U. Tanaka, and K. Nasmyth. 2003. Kinetochore recruitment of two nucleolar proteins is required for homolog segregation in meiosis I. *Dev. Cell.* 4:535–548. doi:10.1016/S1534-5807(03)00086-8

Riedel, C.G., V.L. Katis, Y. Katou, S. Mori, T. Itoh, W. Helmhart, M. Gálová, M. Petronczki, J. Gregan, B. Cetin, et al. 2006. Protein phosphatase 2A protects centromeric sister chromatid cohesion during meiosis I. *Nature.* 441:53–61. doi:10.1038/nature04664

Rock, J.M., and A. Amon. 2009. The FEAR network. *Curr. Biol.* 19:R1063–R1068. doi:10.1016/j.cub.2009.10.002

Sakuno, T., and Y. Watanabe. 2009. Studies of meiosis disclose distinct roles of cohesion in the core centromere and pericentromeric regions. *Chromosome Res.* 17:239–249. doi:10.1007/s10577-008-9013-y

Sampath, S.C., R. Ohi, O. Leismann, A. Salic, A. Pozniakowski, and H. Funabiki. 2004. The chromosomal passenger complex is required for chromatin-induced microtubule stabilization and spindle assembly. *Cell.* 118:187–202. doi:10.1016/j.cell.2004.06.026

Schindler, K., and R.M. Schultz. 2009. The CDC14A phosphatase regulates oocyte maturation in mouse. *Cell Cycle.* 8:1090–1098. doi:10.4161/cc.8.7.8144

Shi, Y. 2009. Serine/threonine phosphatases: mechanism through structure. *Cell.* 139:468–484. doi:10.1016/j.cell.2009.10.006

Shonn, M.A., R. McC Carroll, and A.W. Murray. 2000. Requirement of the spindle checkpoint for proper chromosome segregation in budding yeast meiosis. *Science.* 289:300–303. doi:10.1126/science.289.5477.300

Shou, W., J.H. Seol, A. Shevchenko, C. Baskerville, D. Moazed, Z.W. Chen, J. Jang, A. Shevchenko, H. Charbonneau, and R.J. Deshaies. 1999. Exit from mitosis is triggered by Tem1-dependent release of the protein phosphatase Cdc14 from nucleolar RENT complex. *Cell.* 97:233–244. doi:10.1016/S0092-8674(00)80733-3

Stegmeier, F., and A. Amon. 2004. Closing mitosis: the functions of the Cdc14 phosphatase and its regulation. *Annu. Rev. Genet.* 38:203–232. doi:10.1146/annurev.genet.38.072902.093051

Sullivan, M., and D.O. Morgan. 2007. Finishing mitosis, one step at a time. *Nat. Rev. Mol. Cell Biol.* 8:894–903. doi:10.1038/nrm2276

Tang, Z., H. Shu, W. Qi, N.A. Mahmood, M.C. Mumby, and H. Yu. 2006. PP2A is required for centromeric localization of Sgo1 and proper chromosome segregation. *Dev. Cell.* 10:575–585. doi:10.1016/j.devcel.2006.03.010

Tóth, A., K.P. Rabitsch, M. Gálová, A. Schleiffer, S.B. Buonomo, and K. Nasmyth. 2000. Functional genomics identifies monopolin: a kinetochore protein required for segregation of homologs during meiosis I. *Cell.* 103:1155–1168. doi:10.1016/S0092-8674(00)00217-8

Virshup, D.M., and S. Shenolikar. 2009. From promiscuity to precision: protein phosphatases get a makeover. *Mol. Cell.* 33:537–545. doi:10.1016/j.molcel.2009.02.015

Visintin, R., E.S. Hwang, and A. Amon. 1999. Cfl1 prevents premature exit from mitosis by anchoring Cdc14 phosphatase in the nucleolus. *Nature.* 398:818–823. doi:10.1038/19775

Westermark, J., and W.C. Hahn. 2008. Multiple pathways regulated by the tumor suppressor PP2A in transformation. *Trends Mol. Med.* 14:152–160. doi:10.1016/j.molmed.2008.02.001

Woodbury, E.L., and D.O. Morgan. 2006. Cdk and APC activities limit the spindle-stabilizing function of Fin1 to anaphase. *Nat. Cell Biol.* 9:106–112. doi:10.1038/ncb1523

Woodruff, J.B., D.G. Drubin, and G. Barnes. 2010. Mitotic spindle disassembly occurs via distinct subprocesses driven by the anaphase-promoting complex, Aurora B kinase, and kinesin-8. *J. Cell Biol.* 191:795–808. doi:10.1083/jcb.201006028

Yang, J., J. Wu, C. Tan, and P.S. Klein. 2003. PP2A:B56epsilon is required for Wnt/beta-catenin signaling during embryonic development. *Development.* 130:5569–5578. doi:10.1242/dev.00762

Yellman, C.M., and D.J. Burke. 2006. The role of Cdc55 in the spindle checkpoint is through regulation of mitotic exit in *Saccharomyces cerevisiae*. *Mol. Biol. Cell.* 17:658–666. doi:10.1091/mbc.E05-04-0336

Yokobayashi, S., and Y. Watanabe. 2005. The kinetochore protein Moa1 enables cohesion-mediated monopolar attachment at meiosis I. *Cell.* 123:803–817. doi:10.1016/j.cell.2005.09.013